

# **The role of microevolution, phenotypic plasticity and bet-hedging in phenological adaptation: A meta-analysis on insect diapause**

## **Summary**

Global change alters selection on phenology, due to rises in temperature means, variability and predictability. Species persistence will depend on how phenology evolves, which may encompass according changes in means, variability (bet-hedging) or plasticity.

We conducted a meta-analysis of arthropod diapause timing across species and climatic gradients. We calculated means and slopes of day length reaction norms for 146 populations in 8 orders. We correlated means and slopes of diapause with mean, variability and predictability of winter onset, which we derived from climate station data.

While timing of diapause and winter onset correlated closely, the slopes were neither explained by winter variability nor by predictability. Insect phenology hence responds readily to mean change, but is vulnerable to altered climate variability and predictability.

Global CO<sub>2</sub> concentrations are rising since 100 years, and the rise is accelerating <sup>1</sup> While some species profit from associated temperature changes and expand their phenology (citation) or range (citation), the majority of species faces higher extinction risks (citation). Climate change thus threatens biodiversity <sup>2,3</sup> and first signs of biodiversity decline are already visible <sup>4</sup>. Rises in mean temperature are hence under intense scrutiny. Mean temperatures are, however, not the only potential cause of biodiversity loss - increasing climate variability imposes further extinction risk <sup>5</sup>. For example, increasing variability changes the thermal performance of ectotherms and represses the thermal optimum <sup>6</sup>. Furthermore, the persistence of extreme events is predicted to increase <sup>7</sup>. While the effects of changing means are well-researched, it is inherently more difficult to quantify and mitigate biodiversity loss by increasing variability.

A common response to climate change is phenological adaptation <sup>8,9</sup>, so common, in fact, that it is a frequently used measure of climate change <sup>10</sup>. Studies of phenological adaptation generally concentrate on spring phenologies, especially of birds <sup>11</sup> and trees <sup>12</sup>, whereas autumn phenology received less attention <sup>13</sup>. The diapause timing of arthropods is one notable exception, as studies of their diapause along latitudinal gradients have been studied since 50 years <sup>14,15</sup>. Phenological change may encompass changes in mean timing <sup>16</sup>, as well as phenotypic plasticity <sup>17</sup> and bet-hedging <sup>18</sup>, and these strategies enable adaptation to different facets of changing environments <sup>19</sup>. Yet, there is very little research on these strategies in climates that may simultaneously change in means, variability and predictability. Here, we tested the predictions that changes in mean conditions are associated with microevolution of mean timing <sup>14</sup>, and that changes in climate variability require the evolution of plasticity or bet-hedging, depending on the predictability of the environment <sup>20</sup>.

We conducted a meta-analysis to estimate the relative extent of microevolution, plasticity and bet-hedging under past changes in climatic conditions. Species that expanded their range (e.g. introduced species) have had to adapt to novel climates, so the reaction norms of populations should segregate with changing climatic backgrounds. We searched the literature for studies that measured photoperiodic reaction norms of arthropods (Fig. 1) along climatic gradients. Our dataset included 26 studies with reaction norms of 146 populations in 8 orders (Table S1, black points in Fig. 2). We correlated means and slopes of these reaction norms with mean winter onset, with winter variability and with winter predictability, which we derived from climate data <sup>21</sup>.

We expected that mean diapause timing evolves such that it maximises geometric mean fitness. In predictable environments this should be the timing that allows for the longest growing season, i.e. mean diapause timing should coincide with winter onset. Because diapause timing and winter onset are on different scales (measured in day length vs. julian days), we first calculated the day length of winter onset. This day length followed a clear latitudinal pattern (Fig. 2b), which would be intuitively expected and has been identified as reason for latitudinal gradients in diapause timing <sup>14,15</sup>. This reasoning is, however, flawed, because the day length gradient decreases below zero after autumnal equinox, and becomes negative in winter (Fig. 4). The gradient is rather explained by the julian day of winter onset, which decreases with latitude (Fig. 2a). The overall effect is a positive day-length – latitude relationship that can be approximated by a linear equation between 20 and 70° N, predicting an optimal shift of day length responses of 51 minutes per 5° latitude. This prediction offers a theory for the historic rule of thumb of Danilevsky <sup>14,15</sup>, which states that mean timing progresses by about 60-90 minutes per 5 degree latitude. Diapause timing indeed followed this rule (Fig. 3a), progressing by 69.6 min (CI: 69.1 - 69.9 min) per 5° N ( $R^2 = 0.62$ ). These results show that Danilevsky's rule is accurate across arthropod orders, because species optimize their diapause timing according to the same physiological background.

As the day of winter onset moves further away from autumnal equinox, the effect of latitude on day length becomes more pronounced, causing an exponential pattern in the latitudinal gradient (Fig. 4). Hence, diapause evolution may become more limiting with increasing latitude. We therefore predict that extinction risks increase with the progression of climate change.

The latitudinal gradient further depends on the thermal threshold which is used to calculate winter onset (Supplementary S3). Temperature thresholds between 7°C and 15°C cause latitudinal

gradients between 0.7h and 1.3h per 5° latitude, and the variance among sites decreases with increasing temperature thresholds. Thermal thresholds vary among species, reflecting differences in thermal niches (citation). Our analysis shows that thermal thresholds predict not only direct extinction risk (citation), but cold-adaptedness also increases the required level of microevolution after latitudinal range expansion, while decreasing the benefit of longitudinal dispersal (due to lack of variance among sites).

We calculated day length of winter onset not only to identify the factors that affect the latitudinal gradient in diapause strategies, but also to test whether diapause timing is optimized to match local conditions. Diapause timing correlated well with day length at winter onset (Fig 3b;  $R^2 = 0.68$ ), though the evolution of critical day length flattened at climates with very early winter onset (Diptera, yellow). The photoperiodic responses thus match our theoretical predictions that maximise fitness, indicating that reaction norms evolved readily to novel climatic conditions. This emphasizes the fitness benefit of diapause timing by photoperiodism, and explains its wide spread among insects<sup>22</sup>. Fitness is not optimized by maximizing the arithmetic mean, but by optimizing the geometric mean; these values are different if the environment is variable<sup>23</sup>. One potential strategy to maximise the geometric mean is to decrease between-years variance by avoiding risks (conservative bet-hedging)<sup>24</sup>. We therefore predicted that mean diapause timing is earlier than suggested by the optimal day length in variable climates. We found however no correlation of mean diapause timing with winter variability ( $R^2 = 0$ ) [should correlate diapause with day length \* variability, todo]. Although predicted by theory<sup>24</sup>, empirical evidence for conservative bet-hedging is rare<sup>23</sup>, and we show that insect diapause is no exception.

[unfinished:]

To test for bet-hedging, we correlated the slopes of the reaction norms with winter variability and predictability. Both winter variability (Fig. 2c) and winter predictability (Fig 2d) varied across the northern hemisphere, but did not correlate with latitude. The slopes in diapause timing were not correlated to either of these climatic variables (both  $R^2 = 0.03$ , Fig. 3c,d), and the interaction did also not explain the slopes ( $R^2 = 0$ ). We hence conclude that variability in diapause timing is not a general bet-hedging traits across insect orders.

Climate variability is an important consideration for species resilience<sup>1,6</sup>. Our results show that species are more vulnerable to changes in variability than to changes in means

## Methods

### 1. Overview

We calculated mean, variability and predictability of winter onset across the northern hemisphere and correlated these climatic variables with diapausing strategies (means and slopes) of 146 arthropod populations.

We calculated winter onset in each year and climate station as the fifth day on which temperatures fall below 10 °C. We then derived mean winter onset across years for each station and used the standard deviation among years to estimate winter variability. To calculate winter predictability, we regressed temperatures of the last 30 days before winter onset for each year. The slope of this regression describes the pace of seasonal change, and the between-years standard deviation of the slope determines whether the rate of change is consistent (predictable) across years.

We then extracted photoperiodic response curves (PRCs) from 26 published studies (146 populations) along with their sampling locations. We calculated four-parameter dose-response curves to obtain estimates of lower and upper diapause limit, critical day length (inflection point of a logit-curve) and slope of the curves. Critical day lengths were then correlated with mean winter onset, and the slope estimates were correlated with winter variability and predictability.

### 2. climate data

#### 2.1. data preparation

We used land surface temperature data from the Global Historical Climatology Network (GHCN-Daily) <sup>21,27</sup>. We extracted daily minimum and maximum temperatures from all climate stations (~12.6 million months with data, ~34,000 stations). We removed all days with incomplete data (either minimum or maximum temperature not recorded), all years in which more than half of the data points was missing, all stations that covered less than 3 years of data, and all stations from the southern hemisphere. This procedure left 10,991,727 months in 26,804 climate stations. We then calculated the average of daily maximum and daily minimum temperature of 3-244 years for each station to obtain an estimate of daily mean temperature.

#### 2.2. winter onset and winter variability

To estimate winter onset in each year and station, we identified cold days with average temperatures below 10°C. We then determined winter onset as the fifth cold day after midsummer. Years in which winter did not arrive according to this definition were excluded, and stations with less than 3 years with winter onset removed. Across all stations with recorded winter onsets, 68.5 % of the years had more than 350 days with data, and 85.1% had more than 300 days with data. Nevertheless, we calculated a weighted mean winter onset and a frequency weighed standard deviation of winter onset to account for differences in reliability. To calculate the day length at winter onset, we used the `daylength` function, supplying mean winter onset and latitude. We obtained 25,340 estimates of winter onset, day length at winter onset and winter variability in the northern hemisphere.

## 2.3 winter predictability

To calculate the predictability of winter based on preceding temperatures, we used the temperature recordings of the last 30 days before winter onset of each year. Years with less than 10 temperature recordings in the month preceding winter were excluded. We regressed daily mean temperature over time with a linear model, and recorded the slope estimate of each year. The standard deviation in slopes was then used as predictability estimate. In total there were 25,136 estimates of predictability based on this method.

## 2.4. sensitivity of climate predictions to temperature threshold

Arthropod thermal requirements vary among species, and our use of a 10°C temperature threshold was an arbitrary decision. It resulted in a global median winter onset around Oct 11, which is within the range of commonly reported phenological windows and threshold values<sup>28,29</sup> We systematically varied the temperature threshold between 5 and 15°C, and the number of days below this threshold between 1 and 10 days.

# 3. Empirical data

## 3.1 Eligibility criteria

In our literature search for diapause reaction norms we concentrated on studies that measure photoperiodic response curves (PRCs) of invertebrates. We excluded marine and intertidal organisms, because corresponding climate estimates were only available for terrestrial systems. Invertebrates with a larval stage in shallow water (e.g. mosquitoes) were nevertheless included. Studies with estimates for less than 3 populations (samples) were excluded, because in these cases the variance would be absorbed by the random term “study”, which was included in the analysis. We also excluded all studies that measured diapause at less than three photoperiods. To maximize sample sizes, we did not restrict our analysis to any geographic location or publication language.

## 3.2. Search strategy

A full description of the search strategy can be found in S5 and is summarized in S4. In short, we conducted two independent literature searches in the Web of Science core collection: First (19.02.2018) we limited the search terms to:

```
(photoperiodic AND (geogr* OR range)) OR (photoperiod* AND latitud*)  
OR (photoperiod* AND longitud*)
```

Secondly (15.06.2018), we used a wider range of search terms,

```
TS = (("day length" OR photoperiod* OR diapaus* OR hibern* OR  
dorman*) AND (geogr* OR "range" OR latitud* OR longitud* OR cline$  
OR clinal))  
OR TI = (("day length" OR photoperiod* OR diapaus* OR hibern* OR  
dorman*) AND "populations"),
```

but filtered the output by arthropod-related terminology. We found 1638 references in the first search, of which we judged 377 potentially relevant, and 62 met all inclusion criteria. In the second search we found 2748 references, with 621 potentially relevant and 74 included articles. For both searches we did a full forward-citation search on all included articles, and we found 13 and 3 further references,

respectively. The search results were largely congruent, and altogether there were 78 useful references (624 populations).

### 3.3 inclusion criteria

We considered only studies with published data (raw data or figures) for further analysis, so we removed 12 articles (179 populations). Within each study we only selected those populations that were tested at more than three day lengths, and which had more than 2 estimates on the sloped part of the population's PRC, because otherwise the dose-response curve analysis would not allow for a meaningful slope estimate. Some PRCs were incomplete but nevertheless eligible for analysis, because the upper and lower limits of diapause could be interpolated from the remaining populations of a study (see below). We only included studies with at least 3 remaining populations. This procedure left 33 studies with 189 populations.

### 3.4. Effect size calculation

One study (7 populations) reported the slope and midpoint directly, and the remaining 32 studies presented the raw data as tables (3 studies) or figures (29 studies). In the latter case we saved the figure as .png file and extracted the data with WebPlotDigitizer Version 3.12<sup>30</sup>. Where necessary, the day length was then rounded or corrected to match the description in materials and methods of the respective study. Y-values that were slightly above 100% or below 0% were set to 100% and 0% respectively.

To estimate the midpoints and slopes we modelled diapause with binomial dose response curves in R<sup>31</sup>. This analysis provides lower and upper bounds of photoperiodic induction (we constrained these to range from 0 to 100%), the slope, and the inflection point where 50 % of the individuals are induced (critical day length), so up to four parameters per slope were estimated. We recorded the standard error along with the estimates of slope, inflection point and upper and lower limits, using the robust sandwich estimation method, which allows deviating from the assumption that residual errors have constant variance<sup>32</sup>.

Detailed information on number of individuals per point estimate was rarely available (22 populations, 7 studies), as sample sizes were either given as population-level means (4 populations, 1 study) or as global average or range (139 populations, 22 studies), or missed entirely (2 studies, 10 populations). We used all data that was provided to weigh the individual points of the PRC. We wish to emphasize that a lack of detailed information should not be confused with a partially unweighted ("vote-count") meta-analysis, because the sample size (populations per study) was always known. Rather, the lack of weighing in the PRC estimates lead to slightly higher standard errors in the estimates, i.e. the missing information occurred on a lower level (points within population) than the level of replication (population).

During analysis we removed 7 studies (21 populations) and 22 further populations, because the fitted curves did no longer match the inclusion criteria. 26 Studies and 146 populations were left.

## 3. Statistical analysis

To obtain estimates of mean winter onset, day length at winter onset, variability and predictability for the study site locations, we averaged the estimates from the 5 closest stations within a 5° radius (weighted by 1/euclidian distance). When the coordinates were not directly provided in the study, we used the coordinates of the quoted town or area. Town and area coordinates were made available by the WikiProject Geographical coordinates and the Geohack tool<sup>33</sup>.

We used binomial mixed-effects models that weighted data points by their inverse variance, using a random structure of "study" nested in "genus" nested in "order" ("species" explained zero variance).

Our strict inclusion criteria ensured that all populations have at least two data points on the sloped part. However, populations with data only at the extremes of the slope (e.g. 5% and 95%) nevertheless resulted in unrealistically low standard errors. The inverse variance, which is needed to determine the weight of each study, hence ranged over 5 orders of magnitude ( $10^0$  -  $10^{-5}$ ), with highest values mostly on the least reliable studies. Constraining the analysis to populations with three data points on the sloped part would bias the selection to populations with flat slopes, while halving the dataset and not fully mitigating the problem. Instead, we capped the inverse variance at 10 times the median inverse variance. This affected 15 populations for the slope estimates and 26 studies for the mean estimates. We repeated all further analyses with uncapped variances, with those points removed to test how this decision biased our results.

We correlated the inflection point (critical day length, CDL) of the PRCs with latitude and day length at winter onset, and with a day length \* variability interaction. The slope estimate was correlated with environmental variability, predictability and its interaction. We then repeated all analyses based only individually on the two most prevalent orders of our datasets (lepidoptera, diptera).

For all analyses we report 1) estimates of the fixed effects along with their Wald-Type confidence intervals; 2) a generalized  $I^2$  value and  $I^2$  values for each nesting level of the random terms<sup>34</sup>); and 3) pseudo- $R^2$  values, defined as  $(\sigma^2_{\text{random-effects model}} - \sigma^2_{\text{mixed-effects model}}) / \sigma^2_{\text{random-effects model}}$ <sup>35</sup>.

#### 4. Further information

The data from the empirical studies was extracted with WebPlotDigitizer version 3.12<sup>30</sup>. For processing the climate variables and statistical models we used Perl version 5.22.1, and R version 3.4.4<sup>31</sup>. The data was manipulated with the packages `textreadr`<sup>36</sup>, `Rcurl`<sup>37</sup>, `data.table`<sup>38</sup>, `imputeTS`<sup>39</sup> and the `tidyverse`<sup>40</sup> packages `readr`<sup>41</sup>, `tidyr`<sup>42</sup>, `dplyr`<sup>43</sup>, `stringr`<sup>44</sup> and `magrittr`<sup>45</sup>.

The day length calculations were performed with the package `geosphere`<sup>46</sup>. The dose-response curve analyses were made with the package `drc`<sup>47</sup>, its standard errors were computed with the packages `sandwich`<sup>32</sup> and `lmtest`<sup>48</sup>, and the mixed-effects models were made with the package `metafor`<sup>49</sup>. We further used the packages `lme4`<sup>50</sup>, `nlme`<sup>51</sup>, `MASS`<sup>52</sup>, and `geomapdata`<sup>53</sup>, but did not include any data derived from these functions in the final version of the manuscript.

The history of this research project (including a full description of all tests and approaches) can be found at [https://github.com/JensJoschi/variability\\_timing](https://github.com/JensJoschi/variability_timing).

## References

1. IPCC. Fifth Assessment Report - Synthesis Report. Available at: <http://www.ipcc.ch/report/ar5/syr/>. (Accessed: 26th September 2018)
2. Wilson, R. J., Gutiérrez, D., Gutiérrez, J. & Monserrat, V. J. An elevational shift in butterfly species richness and composition accompanying recent climate change. *Glob. Change Biol.* **13**, 1873–1887 (2007).
3. Midgley, G. F., Hannah, L., Millar, D., Rutherford, M. C. & Powrie, L. W. Assessing the vulnerability of species richness to anthropogenic climate change in a biodiversity hotspot. *Glob. Ecol. Biogeogr.* **11**, 445–451 (2002).
4. Pounds, J. A. *et al.* Widespread amphibian extinctions from epidemic disease driven by global warming. *Nature* **439**, 161–167 (2006).
5. Bathiany, S., Dakos, V., Scheffer, M. & Lenton, T. M. Climate models predict increasing temperature variability in poor countries. *Sci. Adv.* **4**, eaar5809 (2018).
6. Vasseur, D. A. *et al.* Increased temperature variation poses a greater risk to species than climate warming. *Proc. R. Soc. Lond. B Biol. Sci.* **281**, 20132612 (2014).
7. Lenton, T. M., Dakos, V., Bathiany, S. & Scheffer, M. Observed trends in the magnitude and persistence of monthly temperature variability. *Sci. Rep.* **7**, 5940 (2017).
8. Primack, D., Imbres, C., Primack, R. B., Miller-Rushing, A. J. & Del Tredici, P. Herbarium specimens demonstrate earlier flowering times in response to warming in Boston. *Am. J. Bot.* **91**, 1260–1264 (2004).
9. Bellard, C., Bertelsmeier, C., Leadley, P., Thuiller, W. & Courchamp, F. Impacts of climate change on the future of biodiversity. *Ecol. Lett.* **15**, 365–377 (2012).
10. Parmesan, C. Ecological and Evolutionary Responses to Recent Climate Change. *Annu. Rev. Ecol. Evol. Syst.* **37**, 637–669 (2006).
11. edit me. North American Bird Phenology Program — Citizen Science Central. Available at: <http://www.birds.cornell.edu/citscitoolkit/projects/pwrc/nabirdphenologyprogram/>. (Accessed: 26th September 2018)
12. edit me. USA National Phenology Network | USA National Phenology Network. Available at: <https://www.usanpn.org/home>. (Accessed: 26th September 2018)
13. Gallinat, A. S., Primack, R. B. & Wagner, D. L. Autumn, the neglected season in climate change research. *Trends Ecol. Evol.* **30**, 169–176 (2015).
14. Danilevskii, A. S. Photoperiodism and seasonal development of insects. *Photoperiod. Seas. Dev. Insects* (1965).
15. Bradshaw, W. E. Geography of photoperiodic response in diapausing mosquito. *Nature* **262**, 384–386 (1976).
16. Bradshaw, W. E. & Holzapfel, C. M. Evolutionary Response to Rapid Climate Change. *Science* **312**, 1477–1478 (2006).
17. Nussey, D. H., Postma, E., Gienapp, P. & Visser, M. E. Selection on Heritable Phenotypic Plasticity in a Wild Bird Population. *Science* **310**, 304–306 (2005).
18. Hopper, K. R. RISK-SPREADING AND BET-HEDGING IN INSECT POPULATION BIOLOGY. *Annu. Rev. Entomol.* **44**, 535–560 (1999).



19. Tufto, J. Genetic evolution, plasticity, and bet-hedging as adaptive responses to temporally autocorrelated fluctuating selection: A quantitative genetic model. *Evolution* **69**, 2034–2049 (2015).
20. Cohen, D. Optimizing reproduction in a randomly varying environment when a correlation may exist between the conditions at the time a choice has to be made and the subsequent outcome. *J. Theor. Biol.* **16**, 1–14 (1967).
21. Menne, M. J., Durre, I., Vose, R. S., Gleason, B. E. & Houston, T. G. An Overview of the Global Historical Climatology Network-Daily Database. *J. Atmospheric Ocean. Technol.* **29**, 897–910 (2012).
22. Bradshaw, W. E. & Holzapfel, C. M. Evolution of Animal Photoperiodism. *Annu. Rev. Ecol. Evol. Syst.* **38**, 1–25 (2007).
23. Simons, A. M. Modes of response to environmental change and the elusive empirical evidence for bet hedging. *Proc. R. Soc. Lond. B Biol. Sci.* **278**, 1601–1609 (2011).
24. Starrfelt, J. & Kokko, H. Bet-hedging--a triple trade-off between means, variances and correlations. *Biol. Rev. Camb. Philos. Soc.* **87**, 742–755 (2012).
25. Simons, A. M. Playing smart vs. playing safe: the joint expression of phenotypic plasticity and potential bet hedging across and within thermal environments. *J. Evol. Biol.* **27**, 1047–1056 (2014).
26. Vasseur, D. A. & Yodzis, P. The Color of Environmental Noise. *Ecology* **85**, 1146–1152 (2004).
27. Menne, M. *et al.* Global Historical Climatology Network - Daily (GHCN-Daily), Version 3. 22. (2012).
28. Waldo, J. *et al.* The role of environmental variables on Aedes albopictus biology and chikungunya epidemiology. *Pathog. Glob. Health* **107**, 224–241 (2013).
29. Halkett, F. *et al.* Dynamics of Production of Sexual Forms in Aphids: Theoretical and Experimental Evidence for Adaptive “Coin-Flipping” Plasticity. *Am. Nat.* **163**, E112–E125 (2004).
30. Rohatgi, A. *WebPlotDigitizer*. (2017).
31. R Core Team. *R: A language and environment for statistical computing*.
32. Zeileis. Object-oriented Computation of Sandwich Estimators. *J. Stat. Softw.* **9**, (2006).
33. Dispenser, Kolossus & Manske, M. *Geohack*. (Wikipedia, 2018).
34. I<sup>2</sup> for Multilevel and Multivariate Models [The metafor Package]. Available at: [http://www.metafor-project.org/doku.php/tips:i2\\_multilevel\\_multivariate](http://www.metafor-project.org/doku.php/tips:i2_multilevel_multivariate). (Accessed: 26th September 2018)
35. Raudenbush, S. W. Analyzing effect sizes: Random effects models. in *The handbook of research synthesis and meta-analysis* 295–315 (Russell Sage Foundation, 2009).
36. Rinker, T. W. *textreadr: Read Text Documents into R*. (2017).
37. Duncan Temple Lang and the CRAN team. *RCurl: General Network (HTTP/FTP/...) Client Interface for R*. (2018).
38. Dowle, M. & Srinivasan, A. *data.table: Extension of `data.frame`*. (2017).
39. Moritz, S. *ImputeTS: Time Series Missing Value Imputation*. (2018).
40. Wickahm, H. *tidyverse: Easily Install and Load the 'Tidyverse'*. (2017).
41. Wickham, H., Hester, J. & Francois, R. *readr: Read Rectangular Text Data*. (2017).
42. Wickham, H. & Henry, L. *tidyr: Easily Tidy Data with 'spread()' and 'gather()' Functions*. (2018).
43. Wickham, H., Francois, R., Henry, L. & Müller, K. *dplyr: A Grammar of Data Manipulation*. (2017).

44. Wickahm, H. *stringr: Simple, Consistent Wrappers for Common String Operations*.
45. Bache, S. M. & Wickham, H. *magrittr: A Forward-Pipe Operator for R*. (2014).
46. Hijmans, R. J. *geosphere: Spherical Trigonometry*. (2017).
47. Ritz, C., Baty, F., Streibig, J. C. & Gerhard, D. Dose-Response Analysis Using R. *PLOS ONE* **10**, e0146021 (2015).
48. Zeileis, A. & Hothorn, T. Diagnostic Checking in Regression Relationships. *R News* **2**, 7–10 (2002).
49. Viechtbauer, W. Conducting meta-analyses in R with the metafor package. *J. Stat. Softw.* **36**, 1–48 (2010).
50. Bates, D., Mächler, M., Bolker, B. & Walker, S. Fitting Linear Mixed-Effects Models Using lme4. *J. Stat. Softw.* **67**, (2007).
51. Pinheiro, J., Bates, D., DebRoy, S., Sarkar, D. & Team, R. C. *nlme: Linear and Nonlinear Mixed Effects Models*. (2018).
52. venables, W. . & Ripley, B. D. *Modern Applied Statistics with S*. (Springer, 2002).
53. Lees, J. M. *geomapdata: Data for topographic and Geologic Mapping*. (2012).
54. Chen, Y.-S., Chen, C., He, H.-M., Xia, Q.-W. & Xue, F.-S. Geographic variation in diapause induction and termination of the cotton bollworm, *Helicoverpa armigera* Hübner (Lepidoptera: Noctuidae). *J. Insect Physiol.* **59**, 855–862 (2013).
55. Gomi, T. & Takeda, M. Changes in Life-History Traits in the Fall Webworm within Half a Century of Introduction to Japan. *Funct. Ecol.* **10**, 384–389 (1996).
56. 哲雄後藤 & 徳純真梶. 日本産ナミハダニ *Tetranychus urticae* KOCH の休眠誘起の臨界日長とその地理的変異. 日本応用動物昆虫学会誌 **25**, 113–118 (1981).
57. 健一橋本, 和子飯島 & 賢一小川. モンシロチョウ *Pieris rapae crucivora* Boisduval (チョウ目 : シロチョウ科) の蛹休眠を誘起する光周反応の地理的変異. 日本応用動物昆虫学会誌 **52**, 201–206 (2008).
58. Ito, K. & Nakata, T. Geographical variation of photoperiodic response in the females of a predatory bug, *Orius sauteri* (Poppius) (Heteroptera: Anthocoridae) from northern Japan. *Appl. Entomol. Zool.* **35**, 101–105 (2000).
59. Kimura, M. T. Geographic variation of reproductive diapause in the *Drosophila auraria* complex (Diptera: Drosophilidae). *Physiol. Entomol.* **9**, 425–431 (1984).
60. Kimura, M. T. Adaptations to Temperate Climates and Evolution of Overwintering Strategies in the *Drosophila melanogaster* Species Group. *Evolution* **42**, 1288–1297 (1988).
61. Koveos, D. S., Kroon, A. & Veerman, A. The Same Photoperiodic Clock May Control Induction and Maintenance of Diapause in the Spider Mite *Tetranychus urticae*. *J. Biol. Rhythms* **8**, 265–282 (1993).
62. Kurota, H. & Shimada, M. Geographical variation in photoperiodic induction of larval diapause in the bruchid beetle, *Bruchidius dorsalis*: polymorphism in overwintering stages. *Entomol. Exp. Appl.* **107**, 11–18 (2003).
63. Lankinen, P. Geographical variation in circadian eclosion rhythm and photoperiodic adult diapause in *Drosophila littoralis*. *J. Comp. Physiol. A* **159**, 123–142 (1986).
64. Lankinen, P., Tyukmaeva, V. I. & Hoikkala, A. Northern *Drosophila montana* flies show variation both within and between cline populations in the critical day length evoking reproductive diapause. *J. Insect Physiol.* **59**, 745–751 (2013).
65. Lehmann, P., Lyytinen, A., Piironen, S. & Lindström, L. Latitudinal differences in diapause related photoperiodic responses of European Colorado potato beetles (*Leptinotarsa decemlineata*). *Evol. Ecol.* **29**, 269–282 (2015).

66. Lumme, J. & Oikarinen, A. The genetic basis of the geographically variable photoperiodic diapause in *Drosophila littoralis*. *Hereditas* **86**, 129–141 (1977).
67. Lushai, G. & Harrington, R. Inheritance of photoperiodic response in the bird cherry aphid, *Rhopalosiphum padi*. *Physiol. Entomol.* **21**, 297–303 (1996).
68. Murata, Y., Ideo, S., Watada, M., Mitsui, H. & Kimura, M. T. Genetic and physiological variation among sexual and parthenogenetic populations of *Asobara japonica* (Hymenoptera: Braconidae), a larval parasitoid of drosophilid flies. *EJE* **106**, 171–178 (2013).
69. Musolin, D. L., Tougou, D. & Fujisaki, K. Photoperiodic response in the subtropical and warm-temperate zone populations of the southern green stink bug *Nezara viridula*: why does it not fit the common latitudinal trend? *Physiol. Entomol.* **36**, 379–384 (2011).
70. Nechols, J. R., Tauber, M. J. & Tauber, C. A. Geographical variability in ecophysiological traits controlling dormancy in *Chrysopa oculata* (Neuroptera: Chrysopidae). *J. Insect Physiol.* **33**, 627–633 (1987).
71. Noda, H. (Shimane-ken A. E. S. Geographic variation of nymphal diapause in the small brown planthopper [*Laodelphax striatellus*] in Japan. *JARQ Jpn.* (1992).
72. Paolucci, S., Zande, L. van de & Beukeboom, L. W. Adaptive latitudinal cline of photoperiodic diapause induction in the parasitoid *Nasonia vitripennis* in Europe. *J. Evol. Biol.* **26**, 705–718 (2013).
73. Riihimaa, A., Kimura, M. T., Lumme, J. & Lakovaara, S. Geographical variation in the larval diapause of *Chymomyza costata* (Diptera: Drosophilidae). *Hereditas* **124**, 151–164 (1996).
74. Ryan, S. F., Valella, P., Thivierge, G., Aardema, M. L. & Scriber, J. M. The role of latitudinal, genetic and temperature variation in the induction of diapause of *Papilio glaucus* (Lepidoptera: Papilionidae). *Insect Sci.* **25**, 328–336 (2018).
75. Shimizu, T. & Kawasaki, K. Geographic variability in diapause response of Japanese *Orius* species. *Entomol. Exp. Appl.* **98**, 303–316 (2001).
76. Shintani, Y. & Ishikawa, Y. Transition of Diapause Attributes in the Hybrid Zone of the Two Morphological Types of *Psacotha hilaris* (Coleoptera: Cerambycidae). *Environ. Entomol.* **28**, 690–695 (1999).
77. Shroyer, D. A. & Craig, G. B. Egg Diapause in *Aedes triseriatus* (Diptera: Culicidae): Geographic Variation in Photoperiodic Response and Factors Influencing Diapause Termination. *J. Med. Entomol.* **20**, 601–607 (1983).
78. So, P.-M. & Takafuji, A. Local variation in diapause characteristics of *Tetranychus urticae* Koch (Acarina: Tetranychidae). *Oecologia* **90**, 270–275 (1992).
79. Suwa, A. & Gotoh, T. Geographic variation in diapause induction and mode of diapause inheritance in *Tetranychus pueraricola*. *J. Appl. Entomol.* **130**, 329–335 (2006).
80. Takeda, M. & Chippendale, G. M. Phenological adaptations of a colonizing insect: The southwestern corn borer, *Diatraea grandiosella*. *Oecologia* **53**, 386–393 (1982).
81. Tyukmaeva, V. I., Salminen, T. S., Kankare, M., Knott, K. E. & Hoikkala, A. Adaptation to a seasonally varying environment: a strong latitudinal cline in reproductive diapause combined with high gene flow in *Drosophila montana*. *Ecol. Evol.* **1**, 160–168 (2011).

82. 武氏家. キンモンホソガの休眠に関する研究. 日本応用動物昆虫学会誌 **29**, 198–202 (1985).
83. Urbanski, J. *et al.* Rapid Adaptive Evolution of Photoperiodic Response during Invasion and Range Expansion across a Climatic Gradient. *Am. Nat.* **179**, 490–500 (2012).
84. Vaz Nunes, M., Koveos, D. S. & Veerman, A. Geographical Variation in Photoperiodic Induction of Diapause in the Spider Mite (*Tetranychus urticae*): A Causal Relation between Critical Nightlength and Circadian Period? *J. Biol. Rhythms* **5**, 47–57 (1990).
85. Wang, X.-P. *et al.* Geographic variation in photoperiodic diapause induction and diapause intensity in *Sericanus montelus* (Lepidoptera: Papilionidae). *Insect Sci.* **19**, 295–302 (2012).
86. Yoshida, T. & Kimura, T. M. Relation of the Circadian System to the Photoperiodic Clock in *Drosophila triauraria* (Diptera: Drosophilidae) : An Approach from Analysis of Geographic Variation. *Appl. Entomol. Zool.* **29**, 499–505 (1994).

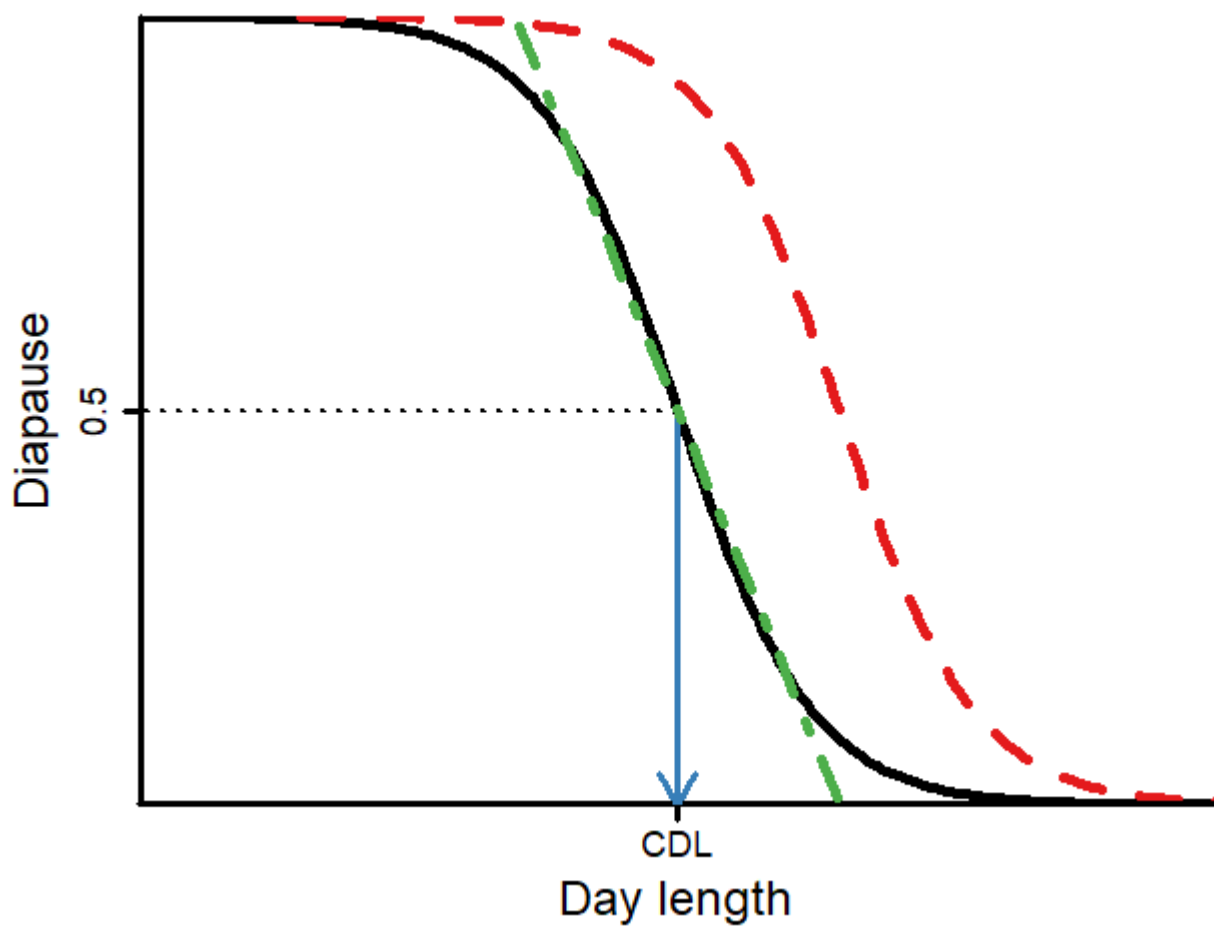


Fig. 1: Hypothetical photoperiodic response curve. The diapausing probability increases with shortening day length (black, solid), and the function follows a logit-curve within physiologically relevant limits. The critical day length (inflection point, blue arrow) and slope (dash-dotted line, green) can be estimated by dose-response curve analysis. Temperature plasticity (dashed, red) leads to a shift on the x-axis.

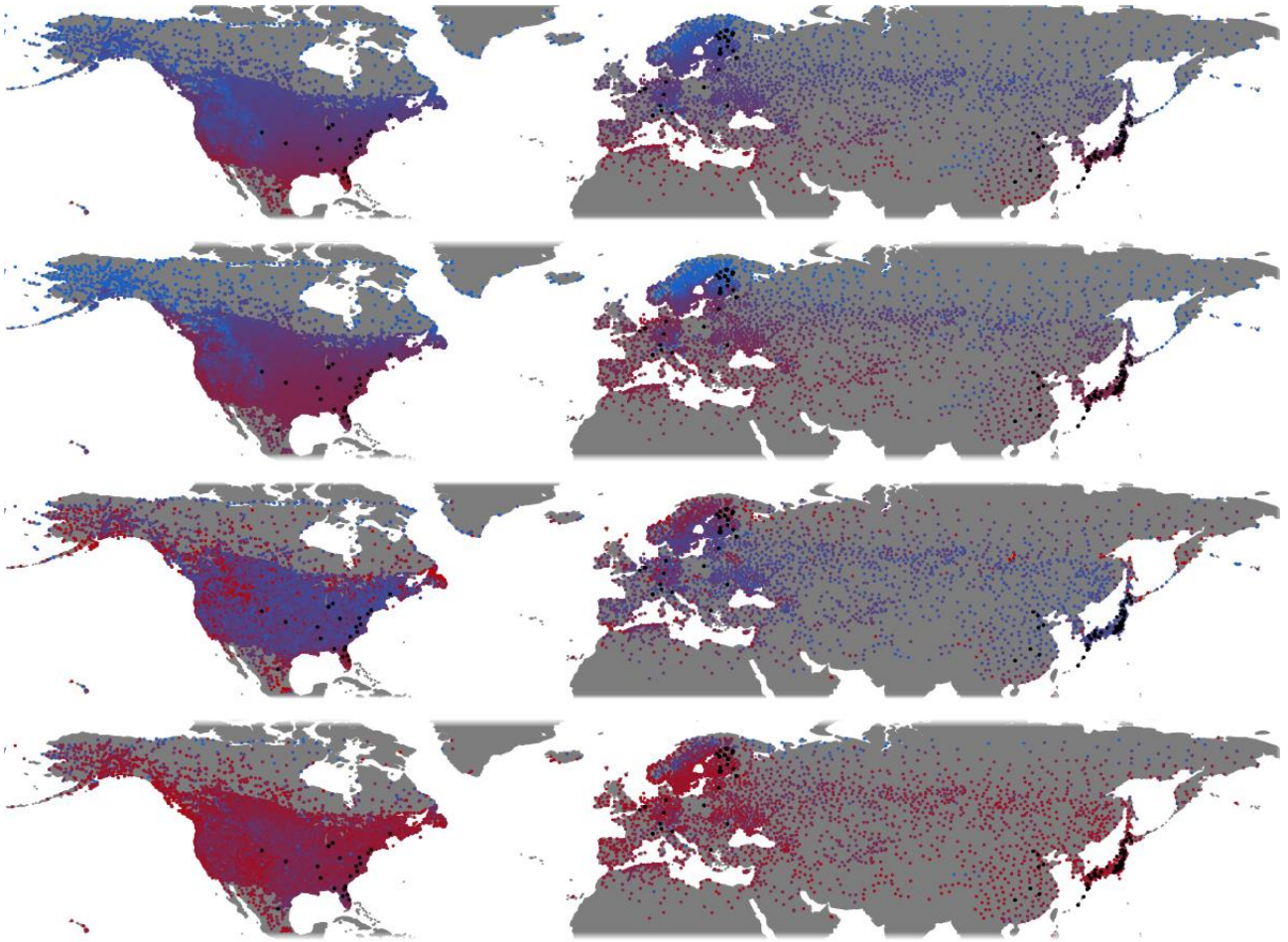
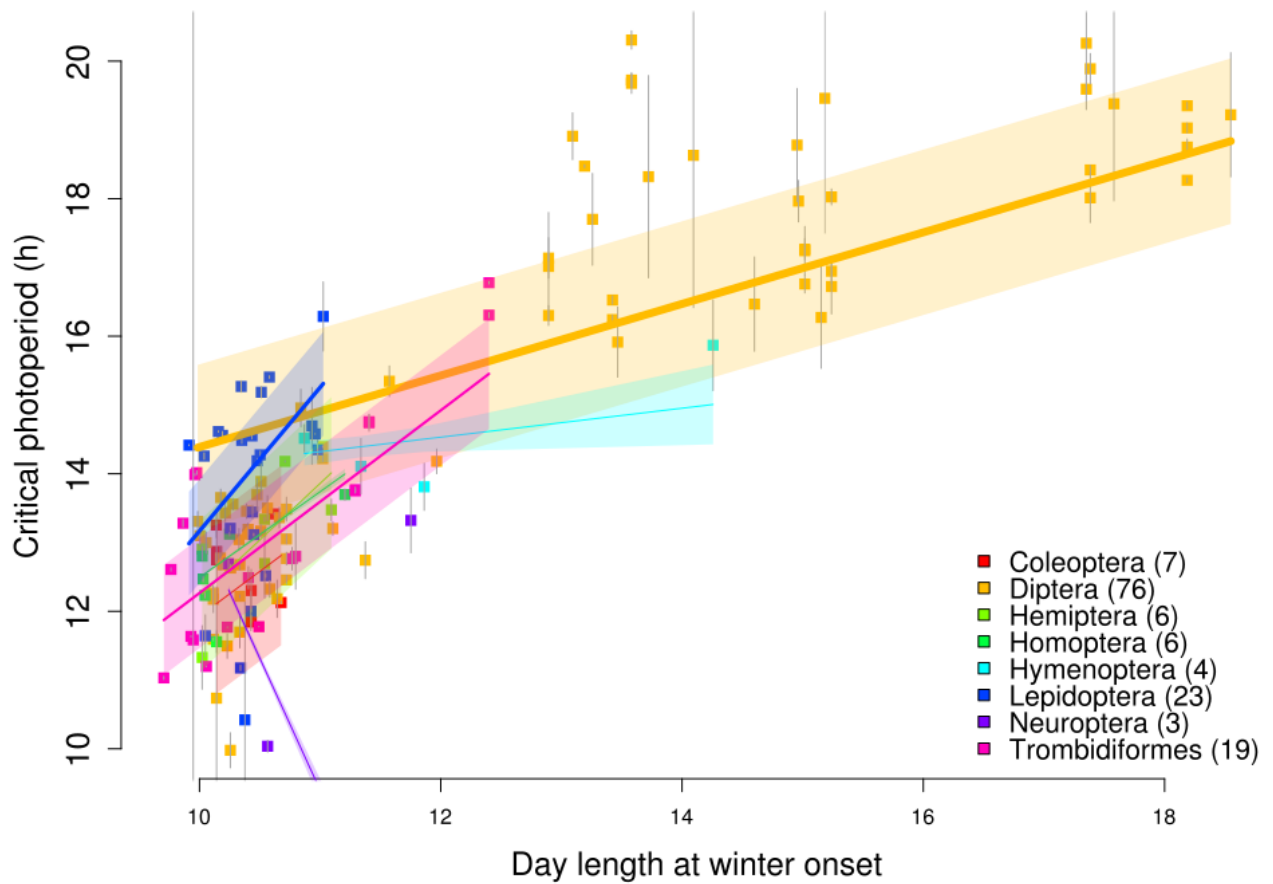
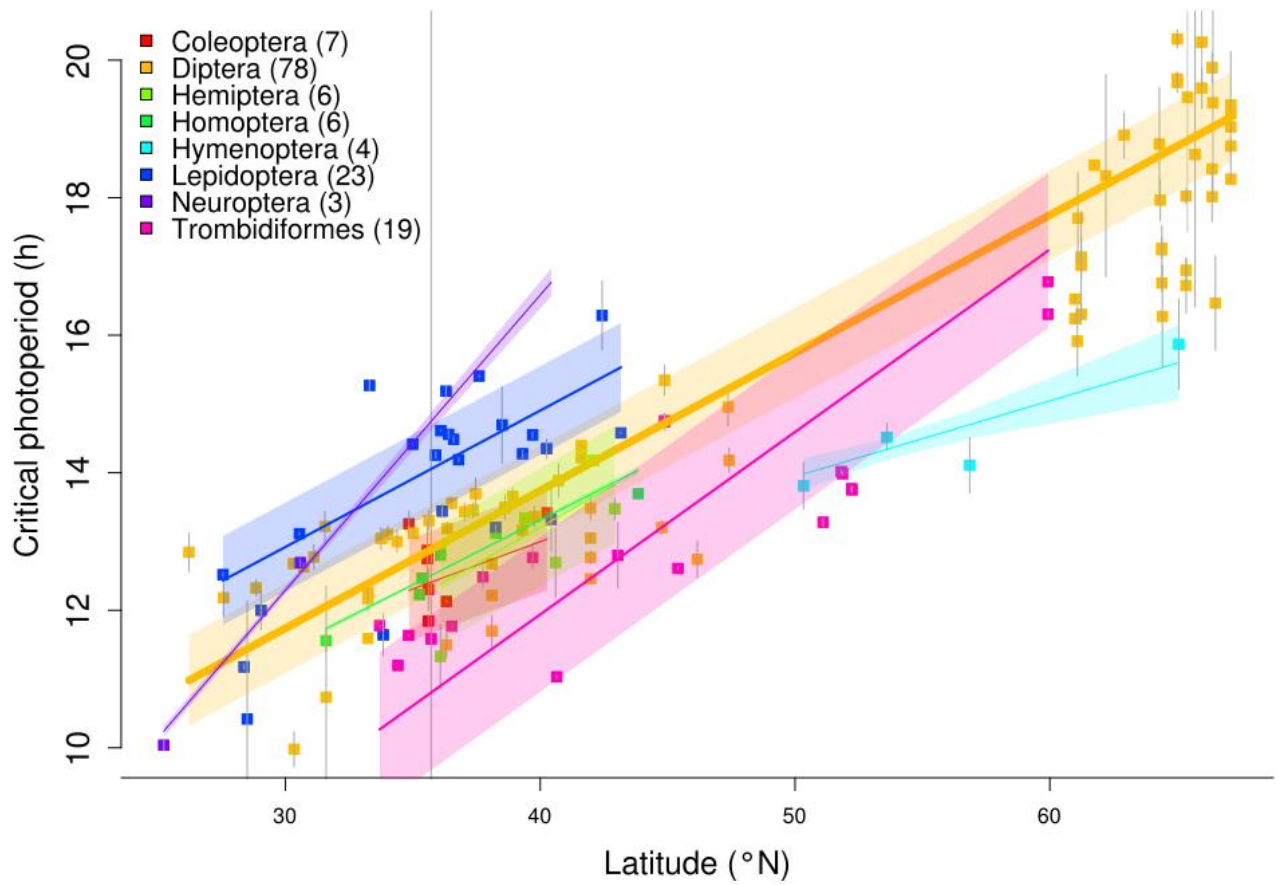


Fig. 2. Mean winter onset (A), day length at mean winter onset (B), winter variability (C) and winter predictability (D) derived from climate data. Winter onset was defined as the 5<sup>th</sup> day after midsummer on which temperatures drop below 10 °C. Winter variability is defined as standard deviation in winter onset. Winter unpredictability was defined as standard deviation in the between-years rate of autumn temperature change (D). Red = late winter onset (A), long day length (B), high variability (C) and high predictability (D) Black points: populations from which reaction norms were extracted.



Caption on next page

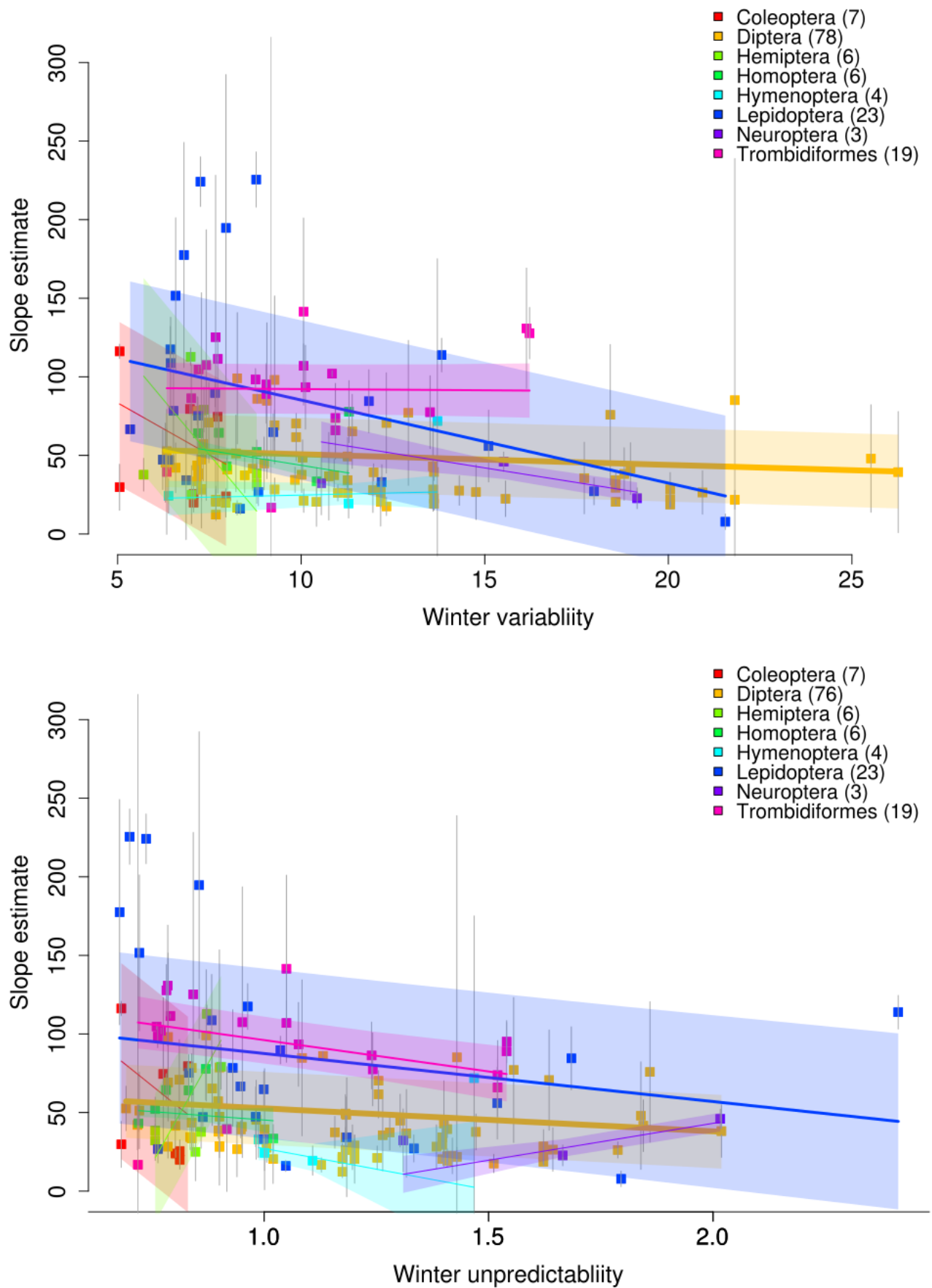


Fig 3. Critical day length vs latitude (a) and vs day length at winter onset (b), and slope estimate vs winter variability (c) and predictability(d). Line width proportional to sample size. Shaded area indicates confidence intervals; grey vertical bars indicate confidence intervals of point estimates.



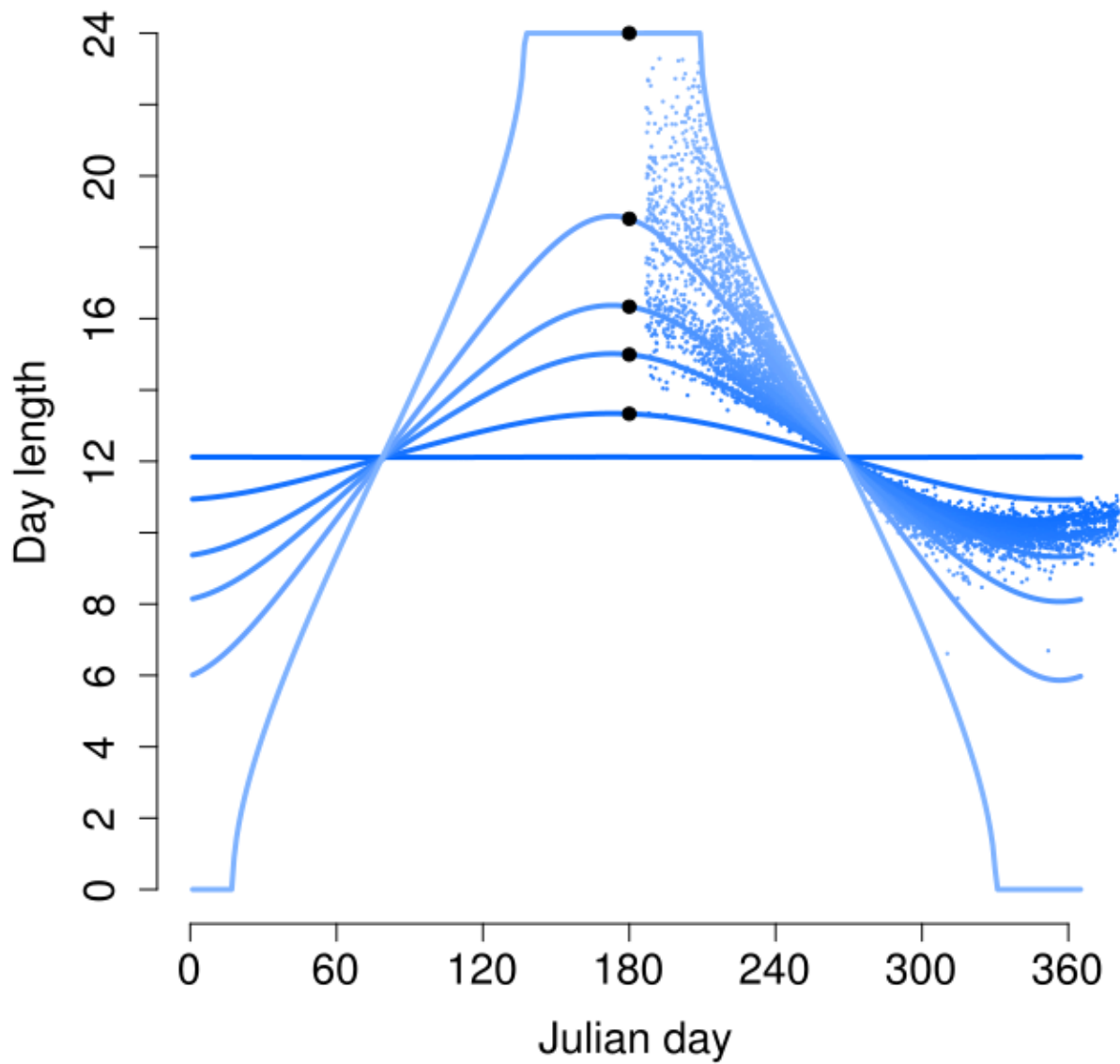
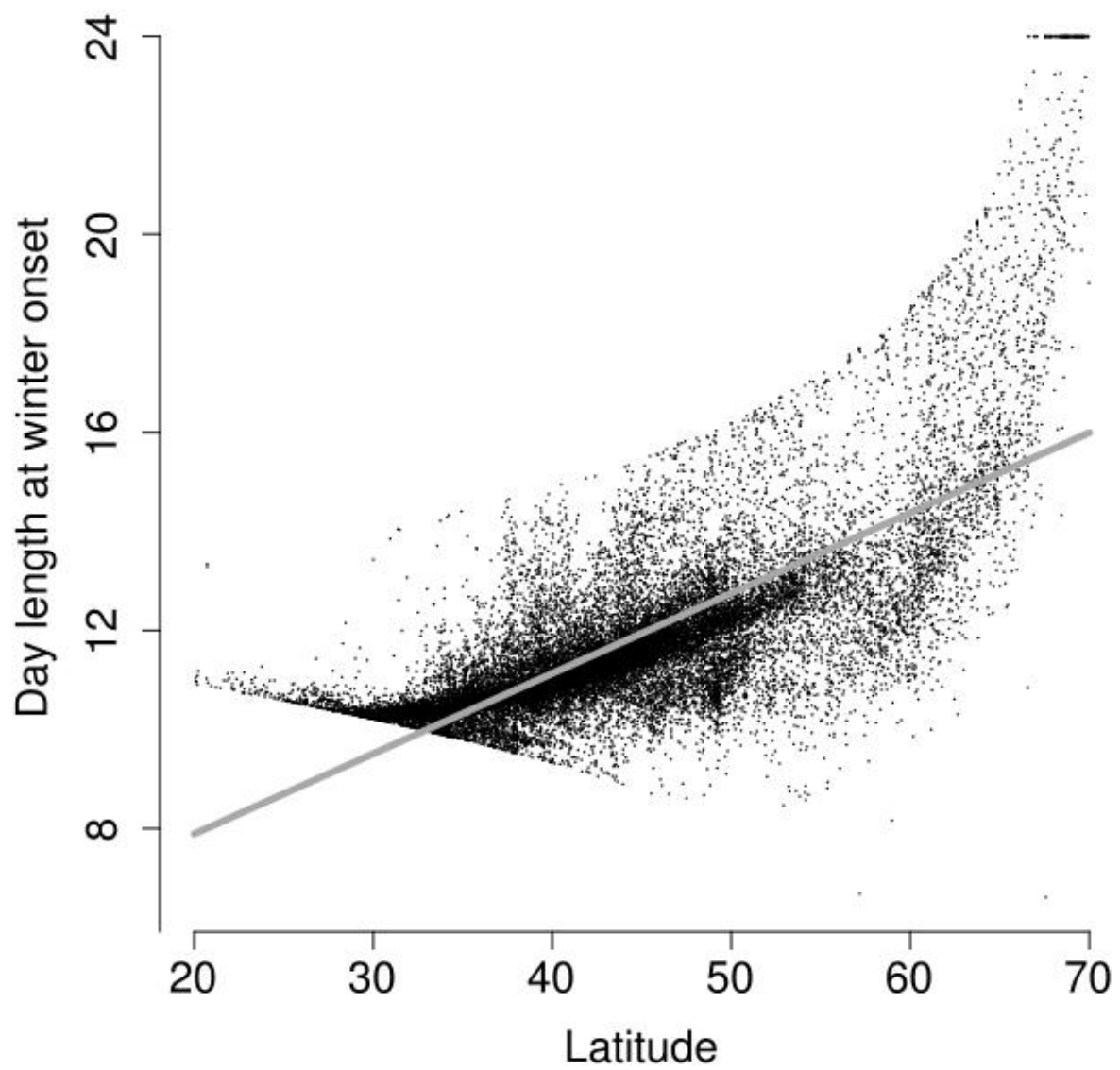


Fig. 4. Day length change as function of day of year. Lines are day length curves for 0°, 20°, 40°, 60° and 70° N. Blue points are day lengths at winter onset derived from 25,340 climate stations (climate data modelling with threshold temperature of 10° C). Shading by latitude is the same as for lines.

Table S1. Studies included in meta-analysis

First Author	Year	Day lengths	Eligible populations	Region	Order	Species
Chen <sup>54</sup>	2013	6	3	China	Lepidoptera	<i>Helicoverpa armigera</i>
Gomi <sup>55</sup>	1996	5	6	Japan	Lepidoptera	<i>Hyphantria cunea</i>
Gotoh <sup>56</sup>	1981	6	4	Japan	Trombidiformes	<i>Tetranychus urticae</i>
Hashimoto <sup>57</sup>	2008	5	6	Japan	Lepidoptera	<i>Pieris rapae</i>
Ito <sup>58</sup>	2000	6	4	Japan	Hemiptera	<i>Orius sauteri</i>
Kimura <sup>59</sup>	1984	8	5	Japan	Diptera	<i>Drosophila auraria</i>
			4	Japan	Diptera	<i>Drosophila triauraria</i>
			3	Japan	Diptera	<i>Drosophila subauraria</i>
Kimura <sup>60</sup>	1988	5	3	Japan	Diptera	<i>Drosophila auraria</i>
Koveos <sup>61</sup>	1993	11	7	Europe	Trombidiformes	<i>Tetranychus urticae</i>
Kurota <sup>62</sup>	2003	6	3	Japan	Coleoptera	<i>Bruchidius dorsalis</i>
Lankinen <sup>63</sup>	1986	7	9	Europe	Diptera	<i>Drosophila littoralis</i>
Lankinen <sup>64</sup>	2013	7	7	Europe	Diptera	<i>Drosophila montana</i>
Lehmann <sup>65</sup>	2015	6	3	Europe	Coleoptera	<i>Leptinotarsa</i>
						<i>decemlineata</i>
Lumme <sup>66</sup>	1977	14	3	Europe	Diptera	<i>Drosophila littoralis</i>
Lushai <sup>67</sup>	1996	10	3	Europe	Hemiptera	<i>Rhopalosiphum padi</i>
Murata <sup>68</sup>	2009	5	3	Japan	Hymenoptera	<i>Asobara japonica</i>
Musolin <sup>69</sup>	2011	6	3	Japan	Hemiptera	<i>Nezara viridula</i>
Nechols <sup>70</sup>	1987	5	3	US	Neuroptera	<i>Chrysopa oculata</i>
Noda <sup>71</sup>	1992		7	Japan	Homoptera	<i>Laodelphax striatellus</i>
Paolucci <sup>72</sup>	2013	8	4	Europe	Hymenoptera	<i>Nasonia vitripennis</i>
Riihimaa <sup>73</sup>	1996	8	4	Europe	Diptera	<i>Chymomyza costata</i>
Ryan <sup>74</sup>	2018	9	3	US	Lepidoptera	<i>Papilio glaucus</i>
Shimizu <sup>75</sup>	2001	7	4	Japan	Hemiptera	<i>Orius sauteri</i>
Shintani <sup>76</sup>	1999	4	4	Japan	Coleoptera	<i>Psacotheta hilaris</i>
Shroyer <sup>77</sup>	1983	9	3	US	Diptera	<i>Aedes triseriatus</i>
So <sup>78</sup>	1992	6	3	Japan	Trombidiformes	<i>Tetranychus urticae</i>
Suwa <sup>79</sup>	2006	5	12	Japan	Trombidiformes	<i>Tetranychus puericula</i>
Takeda <sup>80</sup>	1982	7	3	US	Lepidoptera	<i>Diatraea grandiosella</i>
Tyukmaeva <sup>81</sup>	2011	6	20	Europe	Diptera	<i>Drosophila montana</i>
					Lepidoptera	<i>Phyllonorycter ringoniella</i>
Ujiye <sup>82</sup>	1985	4	3	Japan		
Urbanski <sup>83</sup>	2012	12	21	US, Japan	Diptera	<i>Aedes albopictus</i>
Vaznunes <sup>84</sup>	1990	6	9	Europe	Trombidiformes	<i>Tetranychus urticae</i>
Wang <sup>85</sup>	2012	9	4	China	Lepidoptera	<i>Sericanus montelus</i>
Yoshida <sup>86</sup>	1994	10	3	Japan	Diptera	<i>Drosophila triauraria</i>



Supp. S1 Day length at winter onset as function of latitude

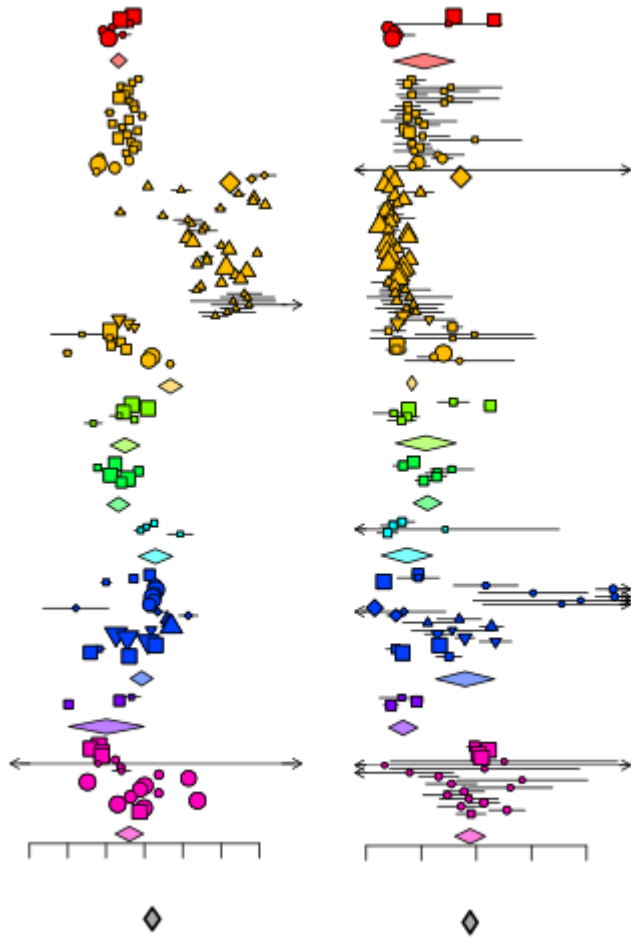


Fig. S2. Forest plot of critical day length (A) and slope (b) estimates. Adjacent points with differing shapes indicate different studies. Error bars indicate confidence intervals of estimates, point size is proportional to inverse of variance. Filled diamonds: order-level means, grey diamond: grand mean Red: Coleoptera; yellow: Diptera; green: Hemiptera; cyan: Homoptera; light blue: Hymenoptera; dark blue: Lepidoptera; violet: Neuroptera; pink: Trombidiformes.

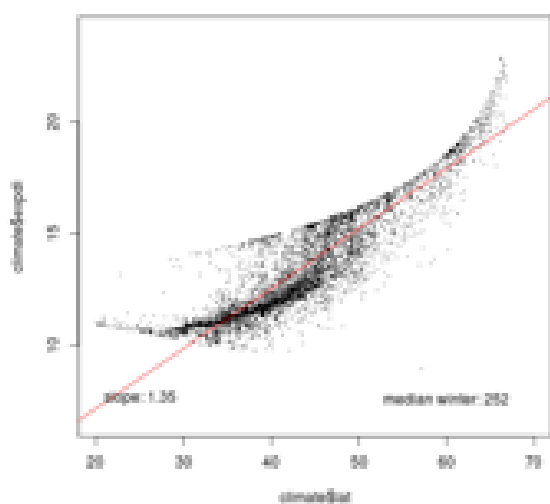
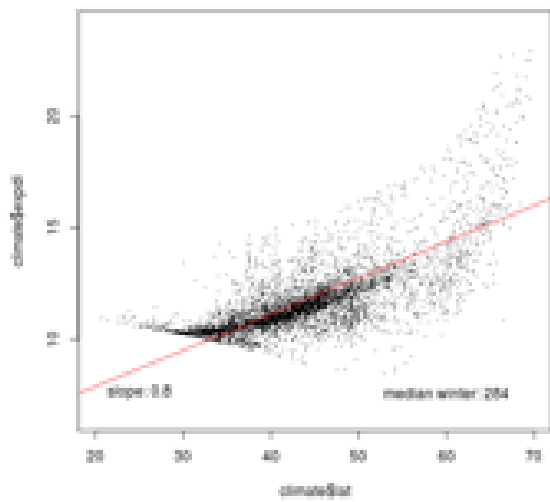
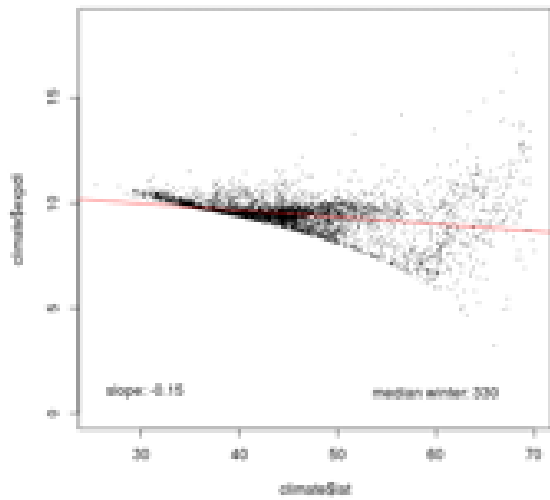


Fig. S3. Placeholder for nice figure. Day length at winter onset vs. latitude for three parameter combinations (temperature thresholds of 0°C, 10° and 15°C. Median winter onset accordingly is at day 300, 284 and day 252. Slopes of linear interpolation are -0.15h, 0.8h and 1.35 h. This figure will be replaced by a 4-panel version of Fig. 4.

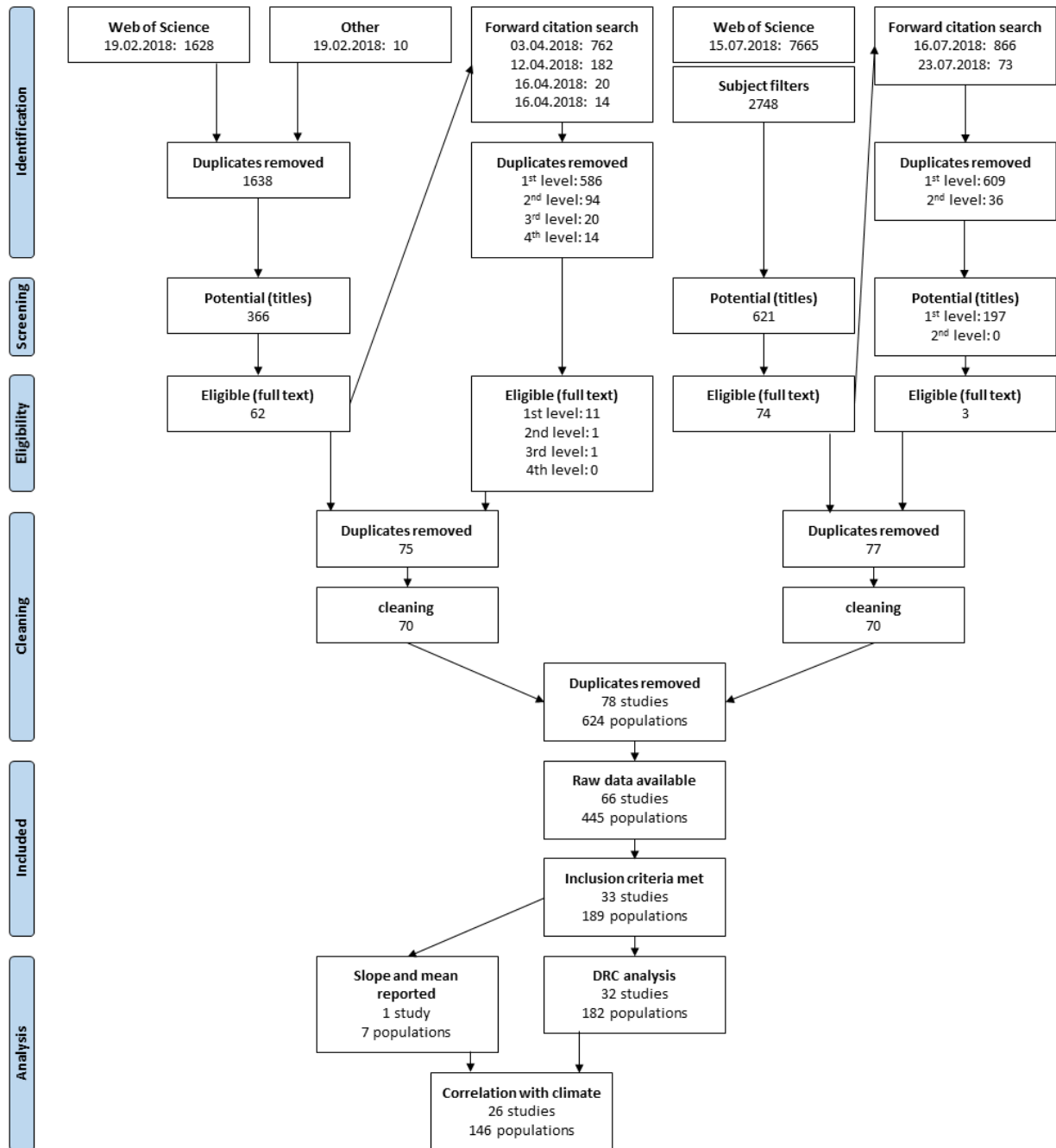


Fig. S4: Search strategy, adapted from the PRISMA(citation) (Preferred Reporting Items for Systematic Reviews and Meta -Analyses) flow chart. Numbers indicate retained datasets.